Evidence for the half-metallic ferromagnetic state of Fe_3O_4 by spin-resolved photoelectron spectroscopy

Yu. S. Dedkov, U. Rüdiger, and G. Güntherodt
II. Physikalisches Institut, Rheinisch-Westfälische Technische Hochschule RWTH Aachen, 52056 Aachen, Germany
(Received 13 September 2001; published 16 January 2002)

The spin-dependent electronic structure of thin epitaxial films of magnetite, $Fe_3O_4(111)$, has been investigated at room temperature by means of spin-, energy-, and angle-resolved photoemission spectroscopy. Near the Fermi energy E_F a spin polarization of $-(80\pm5)\%$ is found. The spin-resolved photoemission spectra for binding energies between 1.5 eV and E_F show good agreement with spin-split band energies from density-functional calculations.

DOI: 10.1103/PhysRevB.65.064417 PACS number(s): 75.70.Ak, 75.50.Bb, 75.70.Cn, 79.60.Bm

The materials class of half-metallic ferromagnets (HMF's) has attracted renewed interest recently in the search for efficient spin polarizers in spin electronics.[1] The intriguing feature of metallic conductivity for one spin component and semiconducting behavior for the other was in most cases theoretically predicted on the basis of electron band structure calculations. An experimental struggle extended over many years and is still ongoing to convincingly verify the truly intrinsic spin-dependent electronic structure of HMF's and consequently the high-spin polarization at the Fermi energy E_F. The use of surface-sensitive measurements like spin-polarized photoemission, tunneling into superconductors, or superconducting point-contact spectroscopy imposed severe constraints in addition to problems with sample stoichiometry and homogeneity. In many cases the preparation of high-quality thin films was indispensable instead of bulk single crystals which are believed to be superior. Thus, from the first theoretical prediction of, e.g., HMF behavior in Heusler alloys in 1983,[2] it took almost two decades to find evidence for spin polarization values at E_F which come close to the expected ones.[3] However, problems with the stoichiometry and especially surface composition of the films used are prevailing.[3–5]

Besides the Heusler alloys, the majority of HMF's have been identified among transition metal oxides on the basis of the local spin-density approximation (LSDA) to the density-functional theory. Predictions have been made for Fe_3O_4,[6,7] CrO_2,[8,9] manganites,[10,11] and the double perovskite Sr_2FeMoO_6.[12] Only recently, values of the spin polarization of over 90% near E_F were found for CrO_2 at 1.8 K using superconducting point-contact spectroscopy,[13,14] although values of 95% had been obtained earlier at 300 K at binding energies of 2 eV below E_F using spin-polarized photoemission.[15] The most straightforward evidence of a minority spin gap and a concomitant 95% spin polarization near E_F was obtained in $La_{0.7}Sr_{0.3}MnO_3$ at 40 K by means of spin-polarized photoemission spectroscopy.[16]

In this paper we present experimental evidence for the half-metallic ferromagnetic state of magnetite (Fe_3O_4) by means of spin- and angle-resolved vacuum ultraviolet (VUV, $h\nu=21.2$ eV) photoemission spectroscopy. Using epitaxial $Fe_3O_4(111)$ films we obtain at room temperature a negative spin polarization of $-(80\pm5)\%$ at E_F. This value agrees within 6% with the magnetization at 300 K of a thin Fe_3O_4 film.[17] More importantly, the spin-resolved photoemission spectra in normal emission along the [111] direction reveal spectral features which are consistent with density-functional calculations of the spin-split electron band energies for binding energies between 1.5 eV and E_F.[7] This result is in contrast to a previous interpretation of photoemission in Fe_3O_4 in terms of an ionic-configuration-based approach and final hole-state effects,[18,19] yielding a maximum value at $T=0$ K of $P=-2/3$ (-66.6%).[20] The epitaxial $Fe_3O_4(111)$ films used in this investigation have been obtained by oxidizing thin (50 Å) epitaxial Fe(110) films by minimum 900 L oxygen exposure ($1\ \mathrm{L}=10^{-6}$ mbar s) followed by post-annealing at 250 °C. The structure of Fe_3O_4 was identified by low-energy electron diffraction (LEED). The magnetic coupling between the $Fe_3O_4(111)$ and underlying Fe(110) layers is found to be parallel, contrary to previous reports.[21]

The experiments were carried out at room temperature in an ultrahigh-vacuum (UHV) system for angle-resolved photoemission spectroscopy with spin analysis described in detail in Ref. 22. It consists of a UHV chamber equipped with a LEED optics, a gas inlet, an Auger electron spectrometer (AES) with a cylindrical mirror analyzer, and a VUV discharge lamp. The unpolarized He I ($h\nu=21.2$ eV) resonance line was used for photoemission experiments. The base pressure in the vacuum chamber was 1×10^{-10} mbar. The spin-resolved photoemission spectra have been recorded in normal emission by a 180° hemispherical energy analyzer connected to a 100-kV Mott detector for spin analysis. The energy resolution was 100 meV and the angle resolution ±3°. The spin-resolved measurements have been performed in magnetic remanence after having applied a magnetic field pulse of about 500 Oe along the in-plane $\langle 1\bar{1}0\rangle$ easy axis of the thin Fe(110) films.[23,24]

The substrate used in this experiment was a 2.5-mm-thick tungsten single-crystal platelet with a diameter of about 7 mm, oriented within 1° along the [110] surface normal direction. Cleaning was achieved by heating at 1800 °C in an O_2 atmosphere of 10^{-6} mbar and flashing up to 2300 °C.

Clean 50-Å-thick Fe(110) films were prepared *in situ* by electron-beam evaporation on a W(110) substrate, while the thickness was simultaneously monitored by a quartz microbalance. The characterization of the growth modes of Fe

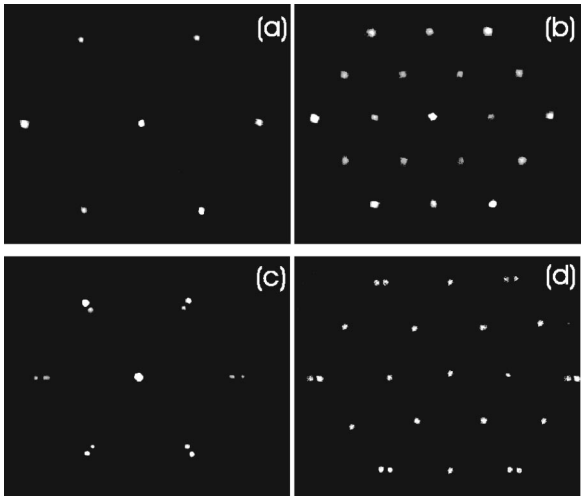

FIG. 1. LEED images of (a) 50 Å Fe(110) film on W(110) substrate and of 50 Å Fe(110)/W(110) after oxidation by (b) 6 L O_2 exposure [resulting in Fe(110)-O-(2×2)/W(110)], (c) 100 L O_2 exposure followed by annealing at $T_{\text{anneal}}=250\,^{\circ}\text{C}$ [resulting in FeO(111)/Fe(110)/W(110)], and (d) 1500 L O_2 exposure with $T_{\text{anneal}}=250\,^{\circ}\text{C}$ [resulting in Fe_3O_4(111)/Fe(110)/W(110)]. The energy of the primary beam is 97 eV for (a) and (b) as well as 123 eV for (c) and 93 eV for (d).

on W(110) has already been reported previously.[25] The degree of crystalline order of the thin epitaxial Fe films used in our experiments has been checked by LEED. In agreement with previous studies[25,26] very sharp (1×1) LEED patterns have been observed [Fig. 1(a)]. The surface cleanliness has been monitored by AES and valence-band photoemission spectroscopy. Different oxygen exposures were accomplished by admitting high-purity gas through a variable-leak valve. Oxygen doses were determined from the ion-gauge reading without any additional correction for oxygen.

The LEED patterns corresponding to the different stages of oxidation of the Fe(110) films are displayed in Figs. 1(b)–1(d). This figure shows LEED images of (b) a $c(2\times2)$-O reconstruction after exposing the clean Fe(110) surface to 6 L of oxygen and of exposures to (c) 100 L O_2 and (d) 1500 L O_2 on Fe(110) with post-annealing at 250 °C. Our results of a $c(2\times2)$ superstructure for 6 L O_2 [Fig. 1(b)] and a $c(3\times1)$ superstructure for 9 L O_2 (not shown in Fig. 1) are consistent with Ref. 26.

After a long exposure of Fe(110) to oxygen with a post-annealing step of the system at 250 °C a hexagonal LEED pattern appears as (1×1) structure for 100 L O_2 [Fig. 1(c)] and as (2×2) superstructure for 1500 L O_2 [Fig. 1(d)]. The appearance of the hexagonal symmetry in the LEED images suggests the formation of a (111)-oriented surface of a fcc lattice. Along the [111] direction the three Fe oxides which are stable under normal conditions—FeO, Fe_3O_4, and α-Fe_2O_3—have similar atomic structures, consisting of (hexagonal) oxygen planes separated by Fe planes. The conditions for the epitaxial growth of well-ordered (111)-oriented Fe oxide layers on Fe(110) substrates were determined in Refs. 21 and 27. These oxides have the following bulk lattice parameters for the (111) surfaces: 2.84, 2.92, and 2.51 Å for FeO, Fe_3O_4, and α-Fe_2O_3, respectively. Assuming ideal bulk-terminated (111) surfaces, previous studies attributed hexagonal (1×1), (2×2), and $(\sqrt{3}\times\sqrt{3})R30°$ LEED patterns to the formation of FeO, Fe_3O_4, and α-Fe_2O_3, respectively.[27] Following these considerations, we attribute the patterns in Figs. 1(c) and 1(d), respectively, to the FeO phase (100 L oxygen exposure) and to the Fe_3O_4 phase (1500 L oxygen exposure). From the LEED images in Figs. 1(c) and 1(d) the following lattice parameters of the (111) planes have been determined: 2.90 ± 0.15 Å for FeO and 3.08 ± 0.15 Å for Fe_3O_4, respectively. These values are somewhat larger than the ones taken from bulk crystallographic data. This is attributed to the lattice mismatch between the epitaxial Fe(110) substrate plane and the epitaxial (111) planes of the Fe oxides (1.5% and 2.0% for FeO and Fe_3O_4, respectively).

Two series of thin iron oxide film preparations have been analyzed in the present work. In the first series we used an ''every-time'' freshly prepared Fe(110) film for each stage of oxygen exposure. In the second series we used a ''one-time'' prepared Fe(110) film for all subsequent oxidation stages. These two series show some differences from a crystallographic point of view. For example, in the second series we observed a hexagonal (1×1) structure after 100 L oxygen exposure and postannealing at 250 °C that corresponds to the formation of a FeO(111) surface. After additional exposure to 200 L oxygen and postannealing at 250 °C we observed a hexagonal (2×2) structure, corresponding to the formation of a Fe_3O_4(111) surface. The same crystallographic structures have been observed in the first series, but only after an extended time of oxygen exposure. We observed a hexagonal (1×1) structure for 100 and 300 L oxygen exposure and a hexagonal (2×2) structure for 900 and 1500 L oxygen exposure.

The spin-resolved photoemission spectra together with the total emission intensity and the spin polarization as a function of binding energy for the first series of oxide films are presented in Figs. 2(a) and 2(b), respectively, for different oxygen exposures $x(L)$. The spin-resolved spectra of the valence band of Fe(110) [bottom curves in Fig. 2(a) for $x=0$ L] show the emission from the $\Sigma^1\downarrow\oplus\Sigma^3\downarrow$ states near 0.25 eV and from the $\Sigma^1\uparrow\oplus\Sigma^4\uparrow$ states near 0.7 eV. The spectra are in agreement with previous measurements.[24,26] The oxidation of Fe(110) is characterized by a gradual decrease in the total intensity of the Fe $3d$ states. The two different oxidation stages of the Fe(110) films shown in Fig. 2(a) for $x=100$ and 900 L are more clearly discernable in the binding energy dependence of the spin polarization in Fig. 2(b). Initially, the oxygen exposure effectively reduces the spin polarization at E_F from $-(83\pm5)\%$ for $x=0$ L to $-(50\pm5)\%$ for $x=100$ L. This is a surprising result because of the antiferromagnetic state of FeO. In a recent paper Koike and Furukawa[28] reported ferromagnetic behavior for FeO(111) layers on Fe(110) with antiparallel coupling between FeO and Fe layers. They found by means of spin-polarized secondary electron spectroscopy a negative spin polarization of -10% of FeO for secondary electrons with zero kinetic energy. The LEED pattern of FeO(111)/Fe(110)

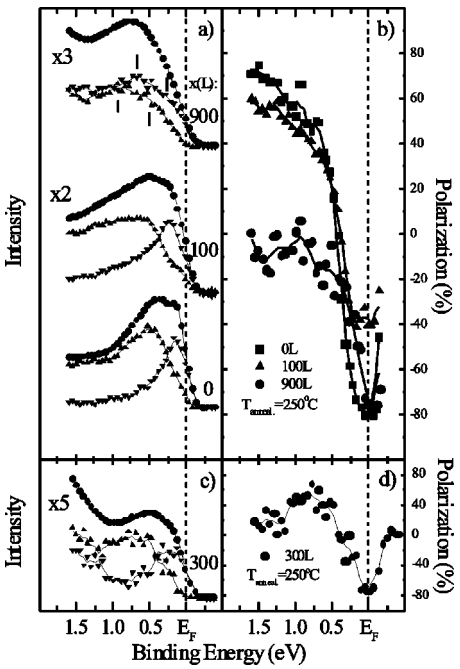

FIG. 2. Oxidation of an ''every-time'' freshly prepared (a), (b) and ''one-time'' prepared (c), (d) 50-Å-thick Fe(110) film at different doses $[x(L)]$ of oxygen after annealing at 250 °C. (a), (c) Spin-polarized photoemission spectra [spin down (down triangle) spin up (up triangle)] and photoemission intensity (circle) and (b), (d) spin polarization as function of binding energy. The thin solid lines through the data points have been obtained by a three-point averaging fast Fourier transformation (FFT) smoothening procedure.

in Ref. 28, however, does not agree with our pattern in Fig. 1(c) and also with the pattern reported by Kim *et al.*[21] The pattern in Fig. 1(b) of Ref. 28 is actually very similar to the one of $Fe_3O_4(111)$ in our Fig. 1(d). Hence we conclude that we are measuring an attenuated spin polarization contribution of the underlying Fe(110) layer.

The attenuation of the spin polarization from the Fe(110) substrate layer by the FeO overlayer was estimated by considering the scattering cross section σ_d of electrons into the four unoccupied *d* orbitals of Fe^{2+} $(3d^6)$ in FeO. We have used the simple rule developed by Siegmann,[29] $\sigma_d = \sigma - \sigma_0$, where σ is the total scattering cross section and σ_0 a constant part. The values were taken from the data compiled in Ref. 29. From the exponential attenuation $P = P_0 \exp(-\sigma_d t)$ we obtain a thickness of the all-Fe overlayer, $t \cong 7$ Å. Considering the oxygen ions intervening the (111) planes of Fe^{2+} ions, the thickness of the FeO overlayer, $t' = 2t/\sqrt{3} \cong 8$ Å, agrees roughly with the expected thickness of FeO.[21,30]

Most surprisingly, an appreciable spin polarization at E_F reappears in Fig. 2(b) for 900 L and above, i.e., for the $Fe_3O_4(111)/Fe(110)$ system. These films show a negative spin polarization at E_F of about $-(80\pm5)\%$ with a parallel magnetic coupling between $Fe_3O_4(111)$ and the underlying Fe(110). However, this polarization value cannot be related anymore to a contribution from Fe(110).

In the work of Kim *et al.*[21] on Fe oxide layers formed on top of thick Fe(110) films, the authors estimated an oxide thickness of 41 and 68 Å for, respectively, 900 and 1500 L oxygen exposures followed by annealing at 250 °C. Hence we attribute the high negative spin polarization for 900 L [Fig. 2(b)] and 1500 L [not shown in Fig. 2(b)] oxygen exposure to an intrinsic property of Fe_3O_4. A similar behavior is found for the second series of films by the successive oxidation of a one-time prepared 50-Å-thick Fe(110) film. In Fig. 2(d) the cumulative result after different oxidation stages is shown for 300 L oxygen exposure followed by post-annealing at 250 °C, yielding a negative spin polarization of $-(80\pm5)\%$. For 50 and 100 L oxygen exposure in this second series the spin polarization of clean Fe(110) had dropped to $-(40\pm5)\%$ [not shown in Fig. 2(d)].

In order to get a rough estimate of the maximal achievable spin polarization at 300 K the spin polarization value of $-(80\pm5)\%$ of our epitaxial Fe_3O_4 films in Figs. 2(b) and 2(d) is compared in first approximation with the temperature dependence of the magnetization $M(T)$ of an epitaxial film of Fe_3O_4 obtained by pulsed-laser deposition on MgO.[17] When extrapolating $M(T)$ to $T=0$ K and normalizing it to $P=-100\%$ we find by scaling $M(T) \sim P(T)$ that the experimental value of $P(300\text{ K})$ is by 6% lower than $M(300\text{ K})$. Such a reduction of the spin polarization near surfaces can be expected due to the excitation of spin waves.[31,32]

In Ref. 21 the rather high photoemission intensity observed near E_F, even at the highest oxygen exposure of 1500 L, was not attributed to the Fe metal underneath, because of the absence of the Fe $3p$ core level spectra. Therefore, as proposed by the authors, it may indicate the formation of an oxygen deficiency near the Fe_3O_4 surface. This may also be responsible for the small positive spin polarization of $+16\%$.[21] It was not possible to obtain a reduced emission intensity at E_F upon exposing the sample to additional oxygen at various temperatures and in a wide oxygen pressure range.

In previous spin-resolved threshold photoemission measurements, i.e., without any energy analysis,[18] a spin polarization of -60% was found for Fe_3O_4 single crystals. However, the spin polarization value by itself is no proof of a half-metallic state as is evident by the above example of Fe(110). Therefore, we have compared features in the spin-resolved photoemission spectra with spin-polarized electron band structure calculations as discussed below.

We conclude that in the photoemission spectra in Figs. 2(a) and 2(c) for $x=900$ and 300 L, respectively, only features of Fe_3O_4 are present with a negligible contribution from the Fe(110) substrate. This is further corroborated by a comparison with the spin-split electron band structure of Fe_3O_4 based on the LSDA to the ''constrained'' density-functional method.[7] As demonstrated in Fig. 2(a), we observed for all oxygen-exposed layers a reduced photoemission intensity near E_F. For the $Fe_3O_4(111)/Fe(110)$ system $(x=900\text{ L})$ the reduction in photoemission intensity near E_F compared to $x=0$ L is for spin-up electrons more than 20 times and for spin-down electrons more than 8 times. This can be interpreted as a band gap formation for spin-up electrons near E_F for both preparation series of $Fe_3O_4(111)/Fe(110)$ [Figs. 2(a) and 2(c)]. Such a spin-up gap is also consistent with the band structure calculation,[7]

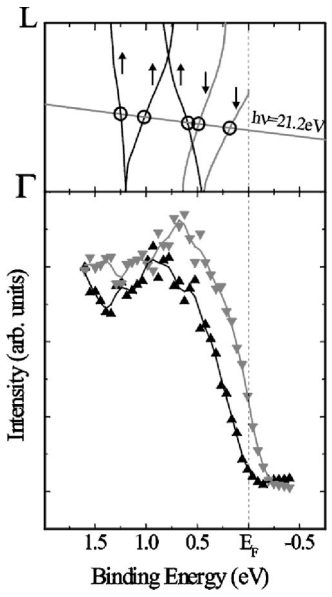

FIG. 3. Lower panel: spin-resolved photoemission spectra of $Fe_3O_4(111)$ for $h\nu=21.2$ eV in normal emission from Fig. 2 [$x(L)=900$]. The lines through the data points have been obtained by a three-point averaging FFT smoothening procedure. Upper panel: spin-split bands of Fe_3O_4 along the Γ-L direction from Ref. 7. The free-electron-like final state has been shifted down by 21.2 eV to yield crossing points indicating the initial states in photoemission.

which shows a 0.45-eV gap for the spin-up electrons below E_F.

The detailed features in the spin-resolved photoemission spectra of $Fe_3O_4(111)$ indicated by tic marks in Fig. 2(a) are compared in Fig. 3 (lower panel) to the band dispersion in Γ-L direction (Fig. 3, upper panel) as calculated in Ref. 7. For the final state in the photoemission using $h\nu=21.2$ eV we assumed a free-electron-like dispersion with a spin-averaged inner potential of 3.5 eV.[27] The downshift of the final-state dispersion by 21.2 eV leads to crossing points with the spin-split conduction bands (Fig. 3, upper panel), which can be related to features in the spin-resolved photoemission spectra (lower panel). The crossing points in the spin-down bands near 0.2 and 0.5 eV correspond to the shoulder near 0.25 eV and the broad maximum near 0.6 eV, respectively, in the spin-down spectrum. In the spin-up bands the crossing points near 0.6, 1.0 and 1.25 eV are related to, respectively, the shoulder near 0.5 eV, the broad maximum near 0.9 eV, and the slight shoulder near 1.25 eV in the spin-up spectrum. The credibility of these assignments is further supported by the tight-binding fit to the linear muffin tin orbital (LMTO) minority bands shown in Ref. 7. The band dispersion is not drastically changed upon going from the Γ point halfway to the L point. The two crossing points in the spin-down bands in the upper panel of Fig. 3 are shifted by 0.1 to 0.2 eV to higher binding energies. The agreement with features in the spin-down spectra is slightly better.

For the successively oxidized Fe(110) film in Fig. 2(c) with $x=300$ L the above-discussed shoulder in the spin-down spectrum near 0.25 eV is more clearly pronounced at the expense of a broad minimum around 0.75 eV. The origin of the latter is presently not yet understood. On the other hand, the shoulder in the spin-up intensity near 0.5 eV in Fig. 2(a) is more pronounced in Fig. 2(c), together with a broad maximum around 0.75 eV. In any case, the spin gap formation in the spin-up spectrum is also clearly seen in Fig. 2(c).

The spin-resolved photoemission spectra of $Fe_3O_4(111)$ for binding energies $1.5\ \text{eV} \leqslant E_b \leqslant E_F$ support the band-type description of the electronic structure of Fe_3O_4. Within this energy interval the photoemission spectra were previously attributed to the ionic-configuration-based transition $^5T_2(3d^6) \rightarrow {}^6A_1(3d^5)+e^-$ of Fe^{2+}, where e^- denotes a photoelectron. The maximum obtainable spin polarization at $T=0$ K of $P=-2/3$ or -66.6% derived in this model,[20] however, cannot account for our experimental finding of $P=-(80\pm5)\%$ at room temperature. Hence we conclude that, despite the importance of electron correlation effects in transition metal oxides, a band-type description of the the electronic structure of Fe_3O_4 seems to be appropriate. Similar band dispersions have been found for $1.0\ \text{eV} \leqslant E_b \leqslant E_F$ for CrO_2 in a LDA+U approach.[9]

In conclusion, our investigation of thin epitaxial $Fe_3O_4(111)$ films at 300 K has shown agreement between spectral features in the spin-resolved photoemission spectra and spin-split energy states of dispersing bands calculated in the LSDA to the ''constrained'' density-functional method. The spin polarization of $P=-(80\pm5)\%$ at E_F is consistent with the magnetization of a thin epitaxial film, except for a small reduction, which can be attributed to the excitation of spin waves near the surface. Thus the experimentally determined spin polarization appears to be almost intrinsic, i.e., independent of artifacts at the surface, such as deviations from stoichiometry, reconstructions, or contaminations. The magnitude of the spin polarization at room temperature, $P=-(80\pm5)\%$, rules out the ionic-configuration-based approach setting an upper limit of $P=-66.6\%$ at $T=0$ K. The agreement of the photoemission spectroscopy in the [111] direction with density-functional calculations, predicting an overall energy gap in the spin-up electron bands in high-symmetry directions, provides evidence for the half-metallic ferromagnetic state of Fe_3O_4.

This work was supported by DFG through Grant No. SFB 341.

[1] W. E. Pickett and J. S. Moodera, Phys. Today **54** (5), 39 (2001).
[2] R. de Groot, F. Müller, P. van Engen, and K. Buschow, Phys. Rev. Lett. **50**, 2024 (1983).
[3] D. Ristoiu, J. P. Nozières, C. N. Borca, T. Komesu, H.-K. Jeong, and P. A. Dowben, Europhys. Lett. **49**, 624 (2000).
[4] C. T. Tanaka, J. Nowak, and J. S. Moodera, J. Appl. Phys. **86**, 6239 (1999).
[5] D. Ristoiu, J. P. Nozières, C. N. Borca, B. Borca, and P. A. Dow-

ben, Appl. Phys. Lett. **76**, 2349 (2000).
[6] A. Yanase and K. Siratori, J. Phys. Soc. Jpn. **53**, 312 (1984).
[7] Z. Zhang and S. Satpathy, Phys. Rev. B **44**, 13 319 (1991)
[8] K.-H. Schwarz, J. Phys. F: Met. Phys. **16**, L211 (1986).
[9] M. A. Korotin, V. I. Anisimov, D. I. Khomskii, and G. A. Sawatzky, Phys. Rev. Lett. **80**, 4305 (1998).
[10] W. E. Pickett and D. J. Singh, Phys. Rev. B **53**, 1146 (1996).
[11] P. K. de Boer, H. van Lenken, R. A. de Groot, T. Rojo, and G. E. Barberis, Solid State Commun. **102**, 621 (1997).
[12] K.-I. Kobayashi, T. Kimura, H. Sawada, K. Terakura, and Y. Tokura, Nature (London) **395**, 677 (1998).
[13] R. J. Soulen, Jr., J. M. Byers, M. S. Osofsky, B. Nadgorny, T. Ambrose, S. F. Cheng, P. R. Broussard, C. T. Tanaka, J. Nowak, J. S. Moodera, A. Barry, and J. M. D. Coey, Science **282**, 85 (1998).
[14] Y. Ji, G. J. Strijkers, F. Y. Yang, C. L. Chien, J. M. Byers, A. Anguelonch, G. Xiao, and A. Gupta, Phys. Rev. Lett. **86**, 5585 (2001).
[15] K. P. Kämper, W. Schmitt, G. Güntherodt, R. J. Gambino, and R. Ruf, Phys. Rev. Lett. **59**, 2788 (1987).
[16] J.-H. Park, E. Vescovo, H.-J. Kim, C. Kwon, R. Ramesh, and T. Venkatesan, Phys. Rev. Lett. **81**, 1953 (1998); Nature (London) **392**, 794 (1998).
[17] G. Q. Gong, A. Gupta, G. Xiao, W. Qian, and V. P. Dravid, Phys. Rev. B **56**, 5096 (1997).
[18] S. F. Alvarado, W. Eib, F. Meier, D. T. Pierce, K. Sattler, H. C. Siegmann, and J. P. Remeika, Phys. Rev. Lett. **34**, 319 (1975).
[19] S. F. Alvarado, M. Erbudak, and P. Munz, Phys. Rev. B **14**, 2740 (1976).
[20] S. F. Alvarado and P. S. Bagus, Phys. Lett. **67A**, 397 (1978).
[21] H.-J. Kim, J.-H. Park, and E. Vescovo, Phys. Rev. B **61**, 15 284 (2000); **61**, 15 288 (2000).
[22] R. Raue, H. Hopster, and E. Kisker, Rev. Sci. Instrum. **55**, 383 (1984).
[23] U. Gradmann, J. Korecki, and G. Waller, Appl. Phys. A: Solids Surf. **39**, 101 (1986).
[24] R. Kurzawa, K.-P. Kämper, W. Schmitt, and G. Güntherodt, Solid State Commun. **60**, 777 (1986).
[25] U. Gradmann and G. Waller, Surf. Sci. **116**, 539 (1982).
[26] H.-J. Kim and E. Vescovo, Phys. Rev. B **58**, 14 047 (1998).
[27] A. Barbieri, W. Weiss, M. A. Van Hove, and G. A. Somorjai, Surf. Sci. **302**, 259 (1994).
[28] K. Koike and T. Furukawa, Phys. Rev. Lett. **77**, 3921 (1996).
[29] H. C. Siegmann, Surf. Sci. **307–309**, 1076 (1994).
[30] S. Masuda, Y. Harada, H. Kato, K. Yagi, T. Komeda, T. Miyano, M. Onchi, and Y. Sakisaka, Phys. Rev. B **37**, 8088 (1988), and references therein.
[31] S. F. Alvarado, Z. Phys. B **33**, 51 (1979).
[32] D. Mauri, D. Scholl, H. C. Siegmann, and E. Kay, Phys. Rev. Lett. **61**, 758 (1988).